BRIEF DEFINITIVE REPORT

Germline deletion of CIN85 in humans with X chromosome–linked antibody deficiency

Baerbel Keller[1]* , Moneef Shoukier[2]* , Kathrin Schulz[3], Arshiya Bhatt[3], Ines Heine[3], Valentina Strohmeier[1], Carsten Speckmann[2], Niklas Engels[3] , Klaus Warnatz[1], and Jürgen Wienands[3]

Ubiquitously expressed Cbl-interacting protein of 85 kD (CIN85) is a multifunctional adapter molecule supposed to regulate numerous cellular processes that are critical for housekeeping as well as cell type–specific functions. However, limited information exists about the in vivo roles of CIN85, because only conditional mouse mutants with cell type–specific ablation of distinct CIN85 isoforms in brain and B lymphocytes have been generated so far. No information is available about the roles of CIN85 in humans. Here, we report on primary antibody deficiency in patients harboring a germline deletion within the *CIN85* gene on the X chromosome. In the absence of CIN85, all immune cell compartments developed normally, but B lymphocytes showed intrinsic defects in distinct effector pathways of the B cell antigen receptor, most notably NF-κB activation and up-regulation of CD86 expression on the cell surface. These results reveal nonredundant functions of CIN85 for humoral immune responses.

Introduction

Expression of a BCR together with its intracellular signal effector proteins is requisite for normal antibody responses in mouse and human (Conley et al., 2009; Durandy et al., 2013). Loss of μ heavy chain or expression of nonfunctional BCR signaling subunits, Ig-α (CD79a) and Ig-β (CD79b), causes agammaglobulinemia, the severest form of antibody deficiency. Alterations in BCR-proximal effector enzymes and their connecting linker proteins can cause different degrees of hypogammaglobulinemia that are usually associated with defective B cell development (Conley et al., 2009; Durandy et al., 2013). Although there is resemblance between mice and humans, the severity of antibody deficiency and the rigorousness with which B cell development is halted upon loss of a given signal protein may differ between mouse mutants and human patients, indicating the existence of species-specific signal redundancies (Conley et al., 2000). This is prominently demonstrated by mutations in the gene for Bruton's tyrosine kinase (Btk), causing X-linked agammaglobulinemia (XLA). In XLA patients, B cells are absent and all Ig isotypes are affected, whereas Btk-deficient mice have reduced B cell numbers, show defects in IgM and IgG3 production, and fail to respond to certain T cell–independent antigens (Rawlings et al., 1993). Btk is required to phosphorylate and thereby activate phospholipase C-γ2 for BCR-induced mobilization of the Ca^{2+} second messenger and

activation of the NF-κB transcription factor. The phosphorylation process occurs within a larger complex that is assembled by the SH2 domain–containing leukocyte protein of 65 kD (SLP65), also called BLNK (Hashimoto et al., 1999; Su et al., 1999; Chiu et al., 2002). Consistent with this is the agammaglobulinemia found in patients that lack SLP65 (Minegishi et al., 1999). SLP65-negative mice show a milder phenotype characterized by poor IgM and IgG3 responses (Jumaa et al., 1999; Pappu et al., 1999; Hayashi et al., 2000; Xu et al., 2000).

It was discovered more recently that SLP65 forms a constitutive complex with Cbl-interacting protein of 85 kD (CIN85; Kometani et al., 2011; Oellerich et al., 2011; Kühn et al., 2016). CIN85 exists in multiple isoforms with cell type–specific expression patterns in almost all tissues (Take et al., 2000; Dikic, 2002). Full-length CIN85, also called Ruk (Gout et al., 2000) or SETA (Bögler et al., 2000; Gout et al., 2000), comprises three N-terminal SH3 domains, a central region with proline-rich SH3 recognition motifs and a C-terminal coiled-coil domain (see Fig. 1 A). Based on protein interaction and colocalization studies, CIN85 has been implicated in several central cell functions including vesicle trafficking, organization of the cytoskeleton, and ubiquitinylation-dependent processes involved in down-modulation of cell surface receptor signaling on many cell

[1]Center for Chronic Immunodeficiency, Medical Center–University of Freiburg, Faculty of Medicine, University of Freiburg, Freiburg, Germany; [2]Institute of Human Genetics, University Medical Center Göttingen, Göttingen, Germany; [3]Institute of Cellular & Molecular Immunology, University Medical Center Göttingen, Göttingen, Germany.

*B. Keller and M. Shoukier contributed equally to this paper; Correspondence to Jürgen Wienands: jwienan@uni-goettingen.de; M. Shoukier's current address is Pränatal Medizin München, Munich, Germany.

A

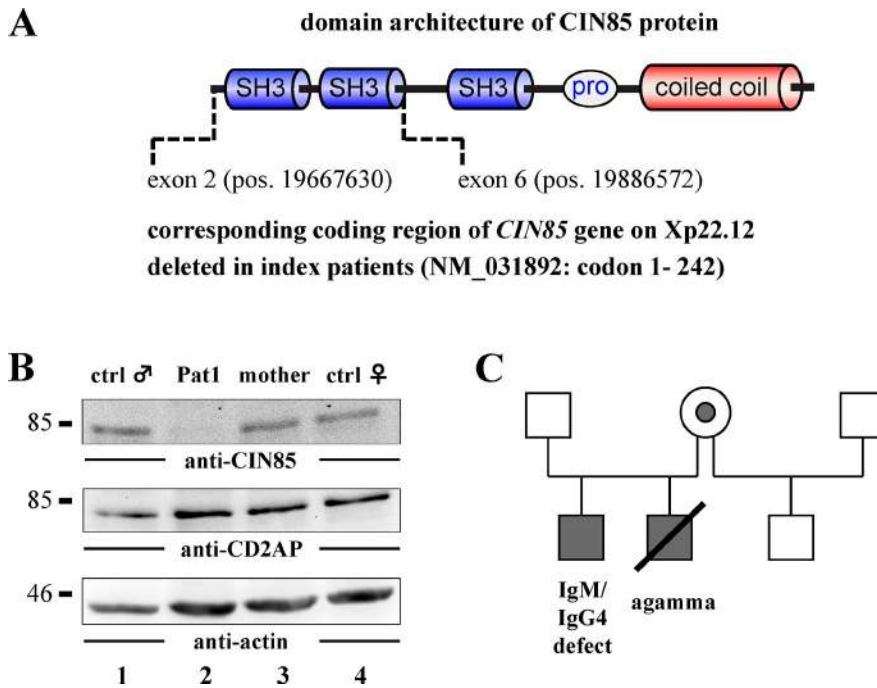domain architecture of CIN85 protein

B

C

Figure 1. **Abrogated expression of CIN85 in antibody-deficient male siblings. (A)** Protein domain architecture of CIN85 and corresponding gene segment that was deleted from chromosome Xp22.12 (position 19667630 to 19886572/GRCh37). SH3, Src homology 3; Pro, proline-rich region; coiled coil region assembles CIN85 trimers. **(B)** Cleared cellular lysates of fibroblasts of a male or female healthy control (lanes 1 and 4), of patient no. 1 (lane 2), or of his mother (lane 3) were subjected to immunoblot analyses with antibodies to CIN85 (upper panel), CD2AP (middle panel), or actin as loading control (lower panel). Relative molecular masses of protein standards are indicated on the left in kD. Please note that working with patients excludes a comprehensive analysis of all organs to formally confirm the complete absence of CIN85 isoforms in all cell types. **(C)** Pedigree of index family. Circles and rectangles indicate females and males, respectively. Fully filled symbols indicate immunodeficient male patients harboring the described *CIN85* deletion on their X chromosome. The partially filled symbol of the patients' mother indicates hemizygosity without clinical symptoms. Strike through indicates death of patient no. 2.

types (Havrylov et al., 2010). Mice with a null mutation in the *CIN85* gene (also called *SH3KBP1)* have not yet been generated. Deletion of CIN85 isoforms in the mouse brain compromised dopamine receptor endocytosis and resulted in hyperactive behavior (Shimokawa et al., 2010). B cell–specific ablation of mouse CIN85 almost blunted IgM and IgG3 responses to Ficoll-coupled hapten, but had little impact on T-dependent antibody responses (Kometani et al., 2011). The B1 cell subset in the peritoneal cavity was drastically reduced, whereas peripheral B2 cell development, including that of marginal zone B cells, was grossly normal. It is conceivable that during B lymphopoiesis and for B cell activation in response to T-dependent antigens, the CIN85-related adapter CD2-associated protein (CD2AP; Dustin et al., 1998; Dikic, 2002) provides some functional redundancy as indicated by RNA interference studies (Oellerich et al., 2011). However, both proteins have been suggested to play key roles in T cell activation via binding to CD2 and the α-chain of the pre–T cell receptor (Dustin et al., 1998; Navarro et al., 2007).

Here we describe two immunodeficient male siblings that harbor an inactivating germline deletion within the *CIN85* gene on the X chromosome. The mutation was accompanied with early onset of severe bacterial infections owing to deficient production of specific antibodies despite the presence of nearly normal B and T cell compartments. The antibody deficiency was traced to specific defects of CIN85-negative B cells in central BCR activation pathways. Our data identify CIN85 as candidate marker for X-linked antibody deficiency.

Results and discussion

Antibody deficiency in two CIN85-negative siblings
Array comparative genomic hybridization (aCGH) was used to determine the genetic defect of 12-yr-old male patient no. 1 with IgM, IgG2, and IgG4 deficiency (Table 1). We detected a

loss of 247.5 kbp in the *CIN85* gene (*SH3KBP1*) on chromosome Xp22.12 of patient no. 1. The deletion encompassed exons 2 to 6 from position 19667630 to 19886572/GRCh37 (see Fig. 1 A), which abrogated CIN85 protein expression of the prevalent transcript NM_031892 (Fig. 1 B, upper panel). *CIN85*-adjacent genes were unaffected. Whole exome sequence analysis did not reveal a phenotypically relevant mutation in 395 genes linked with primary immunodeficiency in humans (Ghosh et al., 2012). Also, expression of CIN85-related CD2AP was normal (Fig. 1 B, middle panel). The mother of patient no. 1 was hemizygous for the *CIN85* deletion that was not found in his healthy half-brother (Fig. 1 C). However, we detected the described *CIN85* deletion in a DNA sample that was isolated from cryoconserved muscle specimens of the brother of patient no. 1 (patient no. 2; Fig. 1 C), who died 3 yr earlier at the age of 15 yr upon a septic shock and multiorgan failure subsequent to a bilateral pneumonia. In patient no. 2, not only serum IgM and IgG2/4 were diminished, but also serum titers of total IgG and IgA were below detection limits.

The IgM/IgG2/4 deficiency of patient no. 1 was associated with bacterial infections, especially during the winter months until his fourth year of life. He overcame this period of severe infections and showed no obvious symptoms of compromised immune reactions ever since. However, his IgG response to pneumococcal polysaccharide vaccination was insufficient against eight of nine serotypes, and also, serotype-specific IgM reached the previously suggested cutoff only for eight of ten serotypes (Table 1). Antipeptide responses exemplified by the anti–tetanus-toxoid response were normal. In marked contrast to patient no. 1, but in accordance with the almost complete absence of all Ig isotypes in the serum, patient no. 2 failed to overcome a juvenile infection period and remained highly susceptible to infection by various pathogens. Repetitive bouts of sinusitis, otitis media, and pneumonia had been reported.

Collectively, we conclude that CIN85 is critical for proper serum Ig levels in humans. CIN85 appears to be indispensable for normal

Table 1. **Immunoglobulin serum levels and anti-PnPS responses in CIN85 deficiency**

	Pat. no. 1	Reference values
	mg/dl	*mg/dl*
Serum IgG4	**<0.8**	5.2–196
Serum IgG3	60	24–116
Serum IgG2	**55**	110–485
Serum IgG1	595	370–910
Serum IgA	79	40–238
Serum IgG	918	672–1,536
Serum IgM	**16**	48–228

	Pat. no. 1 before vaccination	After vaccination	Pat. no. 1 before vaccination	After vaccination
	IgM	IgM	IgG	IgG
	µg/ml	*µg/ml*	*µg/ml*	*µg/ml*
Anti-PnPS type 1	<0.03	**0.13**		
Anti-PnPS type 4	<0.02	**0.22**	0.22	**0.74**
Anti-PnPS type 5	<0.03	1.70	0.31	**0.48**
Anti-PnPS type 6B	0.08	0.46	0.25	**0.42**
Anti-PnPS type 7F	0.06	1.10	0.1	**0.24**
Anti-PnPS type 9V	<0.03	0.12	0.03	**0.66**
Anti-PnPS type 14	<0.08	0.90	<0.03	1.80
Anti-PnPS type 18C	<0.02	0.02	0.16	**0.49**
Anti-PnPS type 19F	0.03	0.14	0.53	**0.58**
Anti-PnPS type 23F	0.01	0.09	0.11	**1.1**

Reference value for serotype specific anti-PnPS IgG ≥1.3 µg/ml. Reference values for IgM anti-PnPS type 1 (1.5 ± 0.4 µg/ml), type 4 (0.9 ± 0.4), and type 14 (0.7 ± 0.4) according to Carsetti et al. (2005). Variations from reference values are indicated in bold.

production of IgM and IgG2/4 classes and antipolysaccharide responses, whereas other class-switched isotypes and antipeptide responses can be generated in the absence of CIN85. The situation resembles the phenotype of conditional mouse mutants with B cell-specific deletion of CIN85, which failed to elicit antibody responses to T-independent type II antigens, but responded normally to T-dependent antigens (Kometani et al., 2011). Additional modifying events, including environmental factors causing the severe presentation of the deceased index patient no. 2, remain unknown because no further material was available for analysis. Clinical heterogeneity among patients with identical mutations is a common phenomenon of primary immunodeficiencies (Conley et al., 2009). Of note, both brothers were diagnosed at the age of 11 yr with moderate attention deficit hyperactivity disability (ADHD), mildly impaired adaptive skills, and obesity. The causative relation of the latter syndromes to CIN85 deficiency remains to be established. However, ADHD of the patients was reminiscent to the physical hyperactivity and explorative behavior of mice lacking the brain isoforms of CIN85 (Shimokawa et al., 2010).

Peripheral B cell compartments develop overtly normal without CIN85

To delineate the immune defect of patient no. 1, we performed a comprehensive flow cytometric characterization of B cell compartments (Table 2). All major B-lymphoid subpopulations including transitional B cells, naive IgM+/IgD+ B cells, CD27+ memory cells, and plasmablasts were present in nearly normal absolute and relative numbers. Hence, CIN85 expression is not mandatory, neither in B-lymphoid cells nor in any other cell types that are relevant for the generation of circulating B cell populations. Similarly, targeted disruption of CIN85 in mouse B cells had little impact on the splenic B2 cell compartment, but reduced the number of IgM-producing peritoneal B1 cells ~7.5-fold (Kometani et al., 2011). The existence and phenotype of the human B1 lineage is controversially discussed (Rothstein and Quach, 2015). However, B1 cells are proposed as a constant source of natural IgM antibody production that is thought to play a crucial role in fighting infection, especially in children with a yet immature immune system (Hardy and Hayakawa, 2015). Provided human B1 cells exist and are similarly dependent on CIN85 expression like mouse B1 cells, their reduction or even absence in patient no. 1 would be consistent with the reduction of serum IgM and his pronounced susceptibility to infections during his early years of life.

CIN85-negative B cells show selective signaling defects

To assess the role of CIN85 for B cell–autonomous activation, we tested the ability of the patient's B cells to respond to various
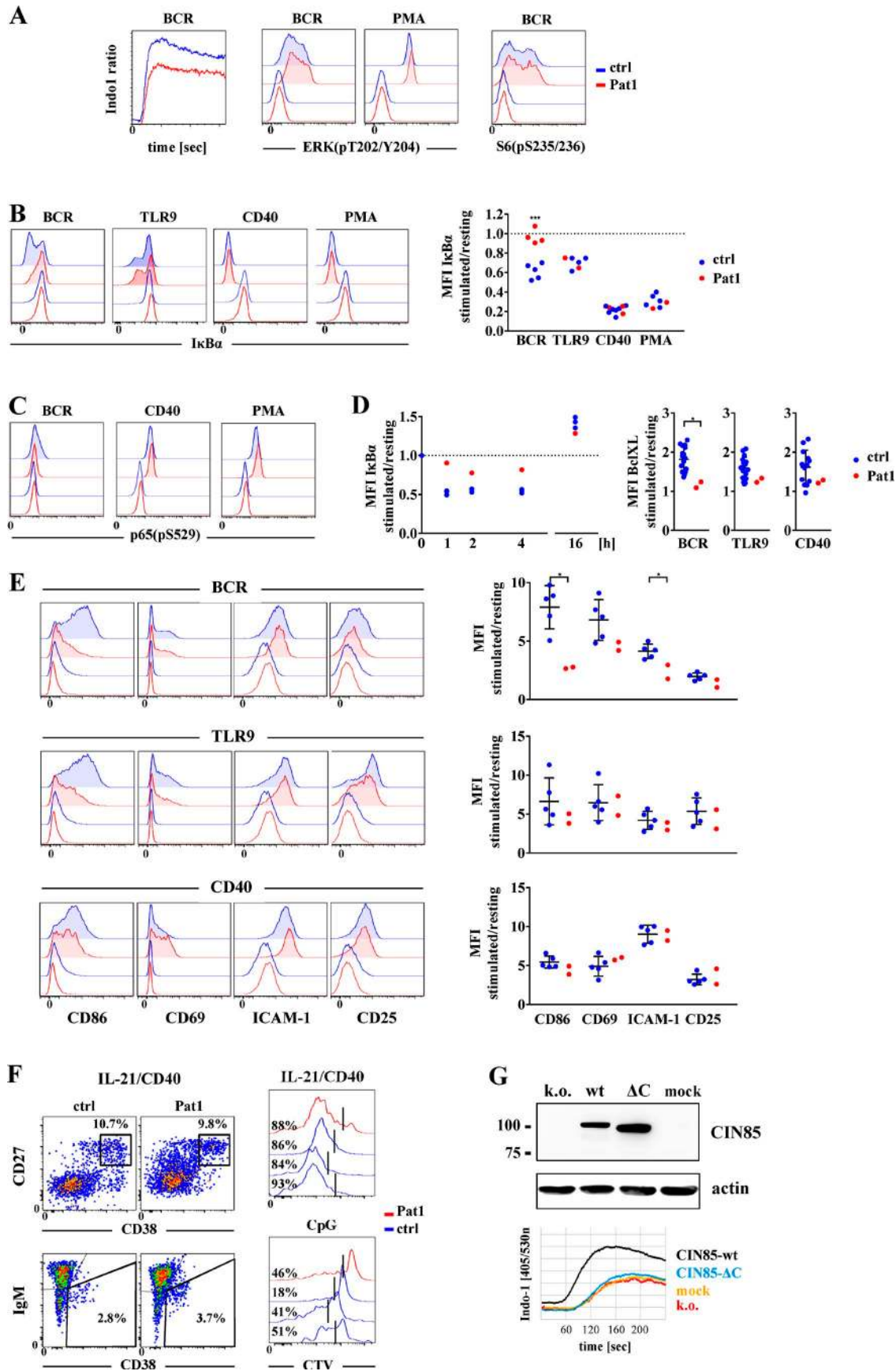
Keller et al.
CIN85 as novel candidate gene for X-linked antibody deficiency

Journal of Experimental Medicine
https://doi.org/10.1084/jem.20170534

1329

Table 2. **Immune cell phenotyping in CIN85 deficiency**

	Pat. no.1	Reference values	Pat no. 1	Reference values
	%	%	cells/μl	cells/μl
Lymphocytes				
CD4	40	30.4–52.9	1,245	608–1,217
CD8	26.2	14–40	815	300–1,300
NK cells	8.7	4–51		
B cells	**5.3**	7.8–23.7	165	119–578
γδ of CD3 T cells	2.4	<10[a]		
CD4 subpopulations				
CD45RA	63	49.2–72	784	311–781
RTE of CD45RA	54.3	33.5–58.2		
T reg	3.1	2.8–7.2	38	25–64
CD8 subpopulations				
Naive	50.7	20–95	413	78–640
Terminally differentiated	**3.7**	9–65	**30**	35–420
Effector memory	9.4	4–100	77	16–810
Central memory	7.0	0.42–18	57	2–86
B cell subpopulations	5.3	7.8–23.7	165	119–578
Transitional B cells	5.9	1.5–7.3	10	2–41
Naive B cells	**83.6**	64.6–80.1	138	83–398
IgM/IgD memory	**4.6**	4.7–15.5	**8**	10–74
IgM only memory	**0.1**	1.6–11.3	**1**	3–39
IgG switched memory	2.5	2.1–9.4	**4**	7–32
IgA switched memory	**1.1**	1.2–3.8	**2**	4–13
Plasmablasts	**0.3**	0.5–4.1[a]		
Kappa/lambda ratio	1.2	1.1–2.0[a]		
CD21^{low}	1.7	1.1–6.9[a]		

Variations from reference values are indicated in bold. RTE, recent thymic emigrants. T reg, regulatory T cells.
[a]Internal diagnostic reference values.

Figure 2. **Ca²⁺ flux and NF-κB signaling deficits of CIN85-negtive B cells. (A)** Ratiometric Ca²⁺ flux kinetics of anti-IgM–stimulated naive B cells of patient no. 1 or healthy control (left panel), and PhosFlow analyses of ERK and S6 phosphorylation in resting (untinted) or activated B cells stimulated through anti-IgM antibodies or PMA (tinted) as indicated. Representative of three (Ca²⁺) or two (ERK and S6) experiments. **(B)** Degradation of IκBα after stimulation of control or patient B cells through BCR, TLR9, CD40, or PMA (four, two, three, and two independent experiments, respectively). For quantification, ratios of the mean fluorescence intensities (MFI) of IκBα after and before B cell stimulation are plotted (right panel). Dotted line indicates no degradation (ratio = 1). **(C)** Phosphorylation of p65 NF-kB subunit after B cell stimulation through BCR, CD40, or PMA treatment. Representative of two experiments. **(D)** Kinetic of IκBα degradation following BCR activation for the indicated time periods in hours (left) and inducible BclXL expression upon activation of BCR, TLR9, or CD40 for 36 h (right). Graphs show MFI ratios of IκBα and BclXL expression after and before B cell stimulation. Reference BclXL MFI values were obtained from 17 healthy controls (two independent experiments). **(E)** Expression of CD86, CD69, ICAM-1, and CD25 (left to right, respectively) upon stimulation of control (blue) or patient (red) B cells through BCR, TLR9, or CD40. For quantification, MFI ratios of the respective surface markers are plotted on the right. **(F)** FACS plots (left panels) of B cell differentiation into CD27-/CD38-positive plasmablasts (upper row) or of class switching from surface IgM to IgG (lower row) upon stimulation of control and patient B cells with IL-21 and anti-CD40 for 8 d. Histograms (right) depict proliferation of naive B cells in response to IL-21/anti-CD40 or CpG stimulation (upper and lower rows, respectively) monitored by cell trace violet (CTV) staining of B cells from three controls or patient no. 1 (two experiments). Vertical lines in histograms indicate gate settings for calculating the percentages of cells that underwent division. If possible, data were analyzed using an unpaired t test. **(G)** Anti-CIN85 and antiactin immunoblot analyses of surface IgM-positive DG75 B cells (upper parts) that were rendered deficient for expression of CIN85 (k.o.) by CRISPR/Cas9 genome editing and of clones expressing citrine-tagged versions of either wild-type CIN85 (wt) or a signaling inactive C-terminal CIN85 deletion mutant (ΔC) or EGFP alone as additional negative control (mock). Relative molecular weights of marker proteins are indicated on the left in kD. Flow cytometric Ca²⁺ mobilization profiles of these cells (lower parts) were recorded upon BCR ligation with 0.5 μg/ml anti-IgM F(ab')₂ fragments (n = 6). Please note that the same results were obtained by an independent second targeting approach using TALEN-mediated CIN85 deletion (data not depicted). Statistically significant differences at p-values of <0.05 (*) or <0.001 (***) are shown.
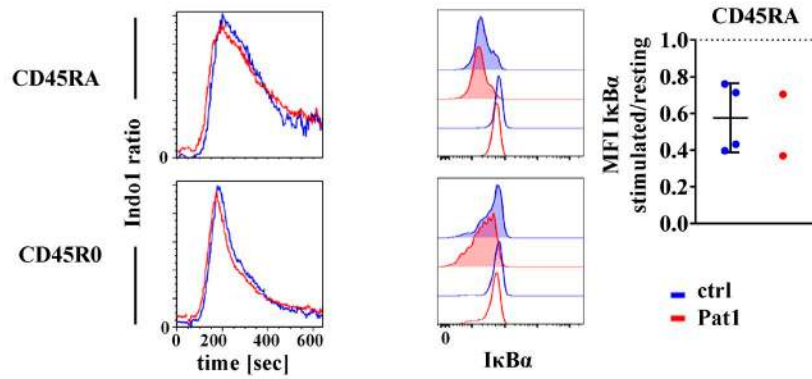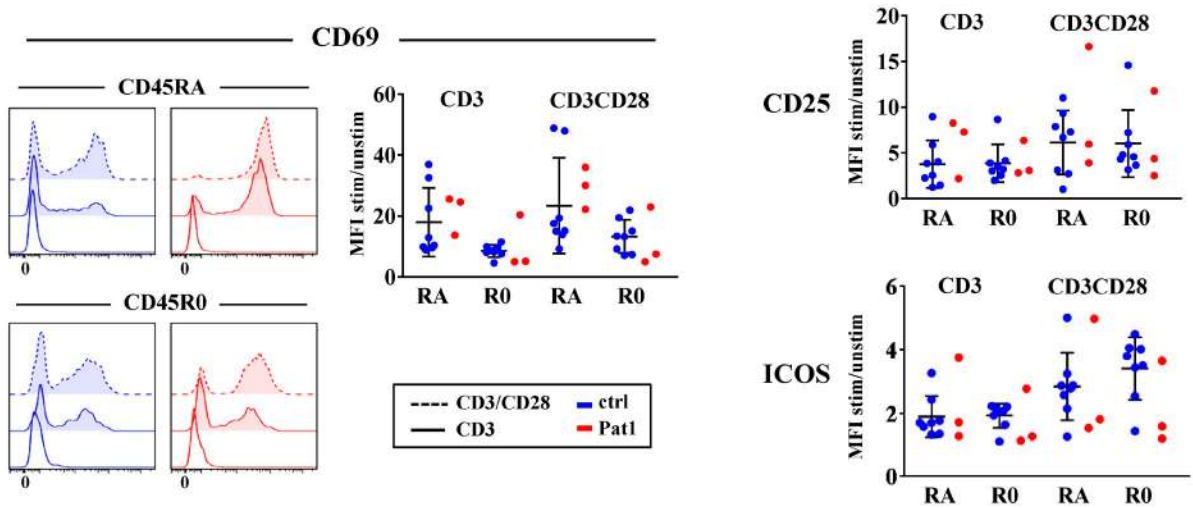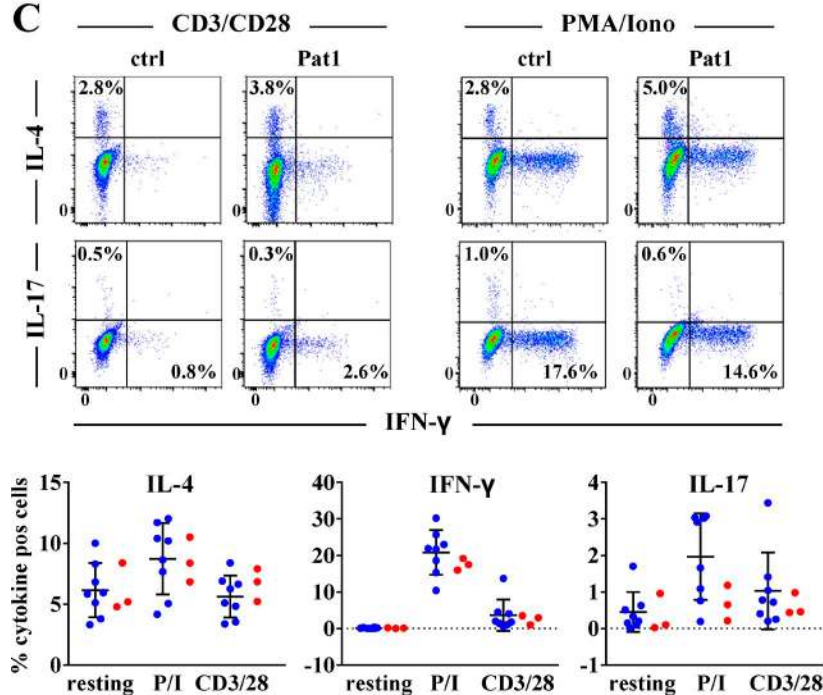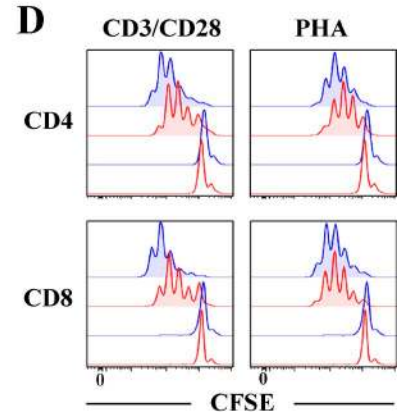
stimuli with mobilization of Ca²⁺, triggering of MAP or PI3 kinases, and induction of the NF-κB pathway. On BCR stimulation, patient B cells consistently showed moderately reduced Ca²⁺ flux compared with healthy control B cells (Fig. 2 A, left) despite even slightly increased BCR surface expression (data not depicted). No differences were observed for inducible ERK phosphorylation, suggesting that the Ras–MAPK pathway was intact in the absence of CIN85 (Fig. 2 A, middle). Normal PI3 kinase activation in the patient's B cells was indicated by robust phosphorylation of the S6 protein (Fig. 2 A, right), which is a downstream target of the Akt–mTOR pathway. Striking differences were, however, observed for BCR-induced NF-κB activation. Although the majority of CIN85 wild-type B cells had degraded the inhibitor IκBα after 40 min upon BCR ligation, only very few B cells of patient no. 1 showed degradation (Fig. 2 B). In contrast, ligation of TLR9 or CD40, as well as treatment of the cells with PMA, activated NF-κB in wild-type and mutant B cells equally well (Fig. 2 B). The reduced degradation of IκBα was reflected by decreased phosphorylation of the p65 subunit, whereas CD40- and PMA-induced p65 phosphorylation was normal (Fig. 2 C). Prolonged BCR stimulation did not substantially enhance degradation of IκBα (Fig. 2 D, left). Accordingly, up-regulation of the NF-κB target gene *BclXL* was compromised upon BCR stimulation, but not upon ligation of TLR9 or CD40 stimulation (Fig. 2 D, right). Hence, CIN85 is indispensable to link BCR ligation to canonical NF-κB activation in human B cells. Surface expression of NF-κB–regulated activation markers CD86, CD69, intercellular adhesion molecule (ICAM)–1 (also known as CD54), and CD25 was measured after stimulation of B cells for 2 d, either through their BCR, TLR9, or CD40 (Fig. 2 E). On CIN85-deficient B cells, BCR-induced CD86 and ICAM-1 up-regulation was diminished, while that of CD69 and CD25 was only moderately affected compared with CIN85-proficient cells. TLR9 and CD40 activation up-regulated all surface markers similarly well on mutant and wild-type B cells. Intact costimulatory signaling in the patient's B cells was confirmed further by the normal in vitro differentiation of plasmablasts and IgG class switching upon IL-21/anti-CD40 stimulation (Fig. 2 F, left). Similarly, proliferation of B cells was within the normal range of healthy controls upon stimulation with IL-21/anti-CD40 or CpG (Fig. 2 F, right). In summary, loss of CIN85 expression in human B cells compromised distinct effector mechanisms of BCR signal transduction that are known to be critical for proper B cell activation. B cell-specific ablation of CIN85 in genetically engineered mice caused the same defects and likewise blocked antibody responses even though

CIN85-proficient T cells are present in mouse mutants (Kometani et al., 2011). A negative regulatory role of CIN85 on BCR signaling suggested by in vitro experiments (Niiro et al., 2012) could not be confirmed in vivo.

Next, we confirmed the positive and nonredundant function of CIN85 for human B cell activation by gene-targeting experiments using the Burkitt's lymphoma line DG75. In addition to CIN85-deficient DG75 cells and as important controls, we also generated clones expressing a signaling-incompetent CIN85 version lacking the C-terminal effector domain (Kühn et al., 2016), as well as cells expressing enhanced GFP (EGFP) instead of CIN85 (Fig. 2 G, upper panel). As observed for primary B cells, loss of wild-type CIN85 strongly compromised BCR-induced Ca²⁺ mobilization (Fig. 2 G, lower panel). Note that the signaling-incompetent version of CIN85 completely failed to restore a normal Ca²⁺ response even though it was slightly more highly expressed than wild-type CIN85. Ca²⁺ flux profiles of all mutant cell populations were almost overlapping. These results reinforce the indispensable role of CIN85 for proper activation of human B cells.

CIN85 is dispensable for the development and functional activation of human T cells

CIN85 and related CD2AP have been implicated in the development and regulation of T cells by binding to CD2 and the pre-TCR α chain (Dustin et al., 1998; Navarro et al., 2007). Hence, we assessed the composition and functionality of the patient's T cell compartments. We found a regular distribution of CD4 and CD8 T cells that were present in normal absolute and relative numbers (Table 2). Also, CD4 subpopulations were normal, including the absolute and relative numbers of naive and memory CD4 T cells, regulatory T cells, and recent thymic emigrants. Similarly, the distribution and numbers of CD8 T cells were normal; only terminally differentiated CD8 cells were slightly reduced. The γ/δ T cell compartment and NK cells were appropriately represented. Hence, T cell development was overtly unaffected by the loss of CIN85. Either CIN85 functions are not essential for the generation of T cell compartments, or those functions can be replaced by other molecules like CD2AP. Patient no. 1's naive and memory CD4 cells mounted normal Ca²⁺ flux and NF-κB activation (Fig. 3 A), as well as S6 phosphorylation (data not depicted) on TCR ligation or TCR/CD28 costimulation. Likewise, CIN85-deficient CD8 cells responded normally (data not depicted). The intracellular T cell signaling competence translated into up-regulation of CD69, CD25, and ICOS (Fig. 3 B). Inducible production of IFN-γ, IL-4, and IL-17 was similar between the patient's and healthy control T

Figure 3. **Robust TCR signaling and T cell function in the absence of CIN85. (A)** Ratiometric Ca²⁺ flux profiles and intracellular staining of IκBα degradation (left and middle panels, respectively) of CD45RA and CD45R0 CD4 T cells (upper and lower rows, respectively) upon anti-CD3/-CD28 stimulation (tinted) or treatment with secondary antibodies alone (unfilled). For quantification, graph on the right depicts MFI ratios of IκBα expression in stimulated and unstimulated CD45RA T cells. Dotted line (ratio = 1) indicates no degradation (two independent experiments). **(B)** Expression of CD69, CD25, and ICOS induced by CD3 or CD3/CD28 stimulation of CD45RA or CD45R0 CD4 T cells from a healthy control or patient no. 1. Representative histograms of inducible CD69 expression are shown on the left where solid and dashed lines indicate anti-CD3 and anti-CD3/-CD28 stimulation, respectively. For quantification, MFI expression ratios of all three T activation markers on naive and memory T cell populations were plotted (middle and right panels; three experiments). **(C)** Intracellular expression of IL-4, IL-17 or IFN-γ in CD45R0 CD4 T cells of patient no. 1 and a control upon TCR/CD28 ligation (upper left four FACS plots) or PMA/Ionomycin treatment (upper right four FACS plots). Quantification (lower three panels) depicts the percentage of positivity for IL-4 (left), IFN-γ (middle), and IL-17 (right) in resting cells, upon PMA/Ionomycin treatment or CD3/CD28 coligation (left to right in each graph; three experiments). **(D)** T cell proliferation monitored by CSFE labeling of CD4 or CD8 T cells (upper and lower panels, respectively) that were obtained from patient no. 1 (red) or a healthy control person (blue) and stimulated via CD3/CD28 or treated with PHA for 5 d (one experiment).

cells (Fig. 3 C). Finally, the proliferation capacity of CD4 and CD8 T cells upon combined stimulation of the TCR and CD28 or treatment with phytohemagglutinin was not significantly affected by the loss CIN85 (Fig. 3 D). It thus appears, that lack of CIN85 has no obvious effect on T cell differentiation and function.

In summary, hypogammaglobulinemia of CIN85-negative patients is unlikely to be caused by insufficient T cell help for antigen-stimulated B cells. Rather, the poor antigen reactivity of B cells appears to be the underlying deficit of this antibody deficiency. In support of that conclusion, expression of a constitutively active version of IKK-β bypassed the need for canonical NF-κB activation in the conditional CIN85 mouse mutant, and importantly, corrected its defective antibody response to T cell–independent type II antigens (Kometani et al., 2011). How exactly CIN85 promotes BCR-induced NF-κB activation remains to be established. However, in association with SLP65, CIN85 supports Ca^{2+} flux and diacylglycerol production which synergistically control the upstream NF-κB regulator PKC-β (Oellerich et al., 2011). NF-κB activation downstream of CD40 and TLR9 appeared to be CIN85-independent as it was largely intact in patient B cells. It is thus conceivable that during T cell–dependent immune responses, the BCR-defective NF-κB activation of patient no. 1 may be compensated for by T helper cell–mediated stimulation of CD40, which allows for the generation of class-switched B cells and the production of Ig-switched isotypes in patient no. 1. The absence of all Ig isotypes in the serum of the deceased brother of patient no. 1 might have been caused by additional genetic and/or epigenetic alterations that were not detectable by exome sequencing. Also, environmental factors can contribute to the known clinical heterogeneity of individual primary antibody deficiencies. In non–B cell types, a large degree of redundancy for CIN85 functions appears to exist that is likely exerted by CD2AP.

Materials and methods

Permissions
All experiments were performed after obtaining parental written informed consent and approval by the institutional review board (FR251/13 and 66/13) following the declaration of Helsinki.

Copy number analysis
An aCGH was performed in the index patient, his half-brother, and their mother using the Agilent SurePrint G3 Human CGH Microarray kit 4_180K (Agilent Technologies) following the manufacturer's instructions. Results were analyzed using Agilent CytoGenomics Edition 2.0.5.0 software and verified by SYBR–green I–based quantitative real-time PCR.

Whole exome sequencing and sequence analysis
Exomes from genomic DNA libraries of human peripheral blood cells were enriched using Illumina TruSeq DNA Sample Prep kit together with Illumina TruSeq Exome Enrichment kit according to the manufacturer's protocol and sequenced on a sequencer (HiSeq 2000; Illumina). Obtained reads were converted into FAS TA-format and aligned against the reference genome assembly

Human_v37_3_dbsnp135_dna using the NextGENe software v 2.3.0 (SoftGenetics). Minimum coverage of five sequencing reads per bp was required for variant calling. Variants present in <15% of the sequencing reads were ignored.

Antibodies
For reference, see Stepensky et al. (2013). Additional antibodies used in the study were TCR αβ FITC, CD3 APC, CD16/CD56 PE, CD8 AF700, CD45RA PE, CD38 Pacific Blue, CD20 PerCp, IgG APC, kappa FITC, lambda PE, CD21 FITC, CD8 PE, and TCR γδ PE (Beckman Coulter GmbH); CD45RA APC-Cy7 and IL-2 PerCpCy5.5 (BioLegend Inc.); CD27 FITC, CD27 APC, CD27 BV605, CD27 PerCpCy5.5, CD38 APC, CD19 APC, IgG PE, S6(pS235/236) APC (BD Biosciences), and IgM AF488 (Jackson); and BclXL AF488 (Cell Signaling Technologies).

Immune cell isolation and intracellular signal transduction
Peripheral blood mononuclear cells (PBMCs) were isolated from EDTA blood by Ficoll density gradient centrifugation and cultured in RPMI 1640 (PAN Biotech), 10% FCS, 1% Penicillin, and 1% Streptomycin at 37°C. For ratiometric Ca^{2+} flux recording by flow cytometry, lymphocytes were labeled with Indo-1, washed, and stained for surface markers of B or T cell subpopulations. Antigen receptors on B and T cells were stimulated with either 10 µg/ml F(ab')$_2$ fragments of anti-IgM antibodies (Southern Biotech) or 5 µg/ml anti-CD3 antibodies (UCHT1; BD Biosciences) for 10 min at room temperature, respectively. The Ca^{2+} baseline level was recorded for 45 s, and ligated antigen receptors were super–cross-linked with 5 µg/ml goat anti–mouse IgG (Jackson). Flow cytometric monitoring of phospho-ERK, phospho-p65, or IκBα was performed after B cell stimulation with 10 µg/ml F(ab')$_2$ anti-IgM, 10 µg/ml anti-CD40 (RandD), 5 µg/ml CpG ODN 2006 (Invivogen), or 200 ng/ml PMA (Sigma). If not mentioned differently, p65 and IκBα were monitored after 40 min of BCR stimulation or 15 min on anti-CD40/PMA treatment. IκBα was analyzed after CpG stimulation for 60 min. ERK phosphorylation was monitored after 5 min, phospho-S6 was determined after 60 min of stimulation. T cell activation was analyzed upon stimulation with 5 µg/ml OKT3 or 5 µg/ml anti-CD28 antibodies (Sanquin) for 30 min on ice, followed by incubation with 5 µg/ml goat anti–mouse IgG for additional 30 min on ice and 60 min at 37°C. Fixed cells were permeabilized using an intracellular staining kit (Phosflow; BD Biosciences) and indicated antibodies. Data acquisition was performed on a LSR Fortessa cell analyzer (BD Biosciences). Targeted disruption of *CIN85* in the IgM-positive human Burkitt's lymphoma cell line DG75 was achieved by genome editing of exon 3 using CRISP/Cas9 technology with single guide RNA selection according to CRISPR Design. Obtained clones were retrovirally reconstituted to express citrine-tagged versions of wild-type CIN85 or a C-terminal CIN85 deletion mutant or EGFP alone.

Lymphocyte activation markers, proliferation, and cytokine secretion
For B cell activation, 5 × 10^6 PBMCs were stimulated with 10 µg/ml anti IgM, 5 µg/ml CpG ODN 2006 (InvivoGen), or 10 µg/ml anti-CD40 (R&D) for 24 h for CD25 and ICAM or 48 h for CD86 and CD69, respectively. BclXL expression was monitored

by intracellular staining upon 36 h of B cell stimulation. T cell activation was performed with 2×10^5 PBMCs, stimulated with immobilized anti-CD3 (OKT3) or anti-CD3/anti-CD28 for 16 h. Cells were harvested and stained with the respective antibodies. B cell proliferation and differentiation was measured after labeling of PBMCs or MACS-isolated naive B cells (Miltenyi; purity >95%) with Cell Trace violet (Life Technologies) following the manufacturers' instructions. Naive B cells were stimulated for 8 d and PBMCs were cultured for 5 d as described previously (Stepensky et al., 2013). T cell activation was performed with 2×10^5 PBMCs and stimulated with immobilized anti-CD3 (OKT3) or anti-CD3/anti-CD28 for 16 h. Cells were harvested and stained with the respective antibodies. For T cell proliferation, PBMCs were labeled with 0.5 µM CFDA/SE (Life Technologies) according to standard protocols. Cells were left untreated or stimulated with 1 µg/ml immobilized anti-CD3 or 0.3 µg/ml anti-CD3 and 0.5 µg/ml soluble anti-CD28 or 2.5 µg/ml PHA (Remel) for 5 d at 37°C. Intracellular cytokines were determined on stimulation of PBMCs with 10 µg/ml anti-CD3 (OKT3) and 2 µg/ml anti-CD28 (Sanquin), or 5 ng/ml PMA and 0.75 µg/ml Ionomycin in the presence of 10 µg/ml Brefeldin A (Sigma-Aldrich). After 6 h, cells were fixed and permeabilized using the BD staining kit for intracellular cytokines according to the manufacturer's instructions.

Acknowledgments

References

Bögler, O., F.B. Furnari, A. Kindler-Roehrborn, V.W. Sykes, R. Yung, H.J. Huang, and W.K. Cavenee. 2000. SETA: a novel SH3 domain-containing adapter molecule associated with malignancy in astrocytes. *Neuro-oncol.* 2:6–15. https://doi.org/10.1093/neuonc/2.1.6

Carsetti, R., M.M. Rosado, S. Donnanno, V. Guazzi, A. Soresina, A. Meini, A. Plebani, F. Aiuti, and I. Quinti. 2005. The loss of IgM memory B cells correlates with clinical disease in common variable immunodeficiency.

J. Allergy Clin. Immunol. 115:412–417. https://doi.org/10.1016/j.jaci.2004.10.048

Chiu, C.W., M. Dalton, M. Ishiai, T. Kurosaki, and A.C. Chan. 2002. BLNK: molecular scaffolding through 'cis'-mediated organization of signaling proteins. *EMBO J.* 21:6461–6472. https://doi.org/10.1093/emboj/cdf658

Conley, M.E., J. Rohrer, L. Rapalus, E.C. Boylin, and Y. Minegishi. 2000. Defects in early B-cell development: comparing the consequences of abnormalities in pre-BCR signaling in the human and the mouse. *Immunol. Rev.* 178:75–90. https://doi.org/10.1034/j.1600-065X.2000.17809.x

Conley, M.E., A.K. Dobbs, D.M. Farmer, S. Kilic, K. Paris, S. Grigoriadou, E. Coustan-Smith, V. Howard, and D. Campana. 2009. Primary B cell immunodeficiencies: comparisons and contrasts. *Annu. Rev. Immunol.* 27:199–227. https://doi.org/10.1146/annurev.immunol.021908.132649

Dikic, I. 2002. CIN85/CMS family of adaptor molecules. *FEBS Lett.* 529:110–115. https://doi.org/10.1016/S0014-5793(02)03188-5

Durandy, A., S. Kracker, and A. Fischer. 2013. Primary antibody deficiencies. *Nat. Rev. Immunol.* 13:519–533. https://doi.org/10.1038/nri3466

Dustin, M.L., M.W. Olszowy, A.D. Holdorf, J. Li, S. Bromley, N. Desai, P. Widder, F. Rosenberger, P.A. van der Merwe, P.M. Allen, and A.S. Shaw. 1998. A novel adaptor protein orchestrates receptor patterning and cytoskeletal polarity in T-cell contacts. *Cell.* 94:667–677. https://doi.org/10.1016/S0092-8674(00)81608-6

Ghosh, S., F. Krux, V. Binder, M. Gombert, T. Niehues, O. Feyen, H.J. Laws, and A. Borkhardt. PID-NET: German Network on Primary Immunodeficiency Diseases. 2012. Array-based sequence capture and next-generation sequencing for the identification of primary immunodeficiencies. *Scand. J. Immunol.* 75:350–354. https://doi.org/10.1111/j.1365-3083.2011.02658.x

Gout, I., G. Middleton, J. Adu, N.N. Ninkina, L.B. Drobot, V. Filonenko, G. Matsuka, A.M. Davies, M. Waterfield, and V.L. Buchman. 2000. Negative regulation of PI 3-kinase by Ruk, a novel adaptor protein. *EMBO J.* 19:4015–4025. https://doi.org/10.1093/emboj/19.15.4015

Hardy, R.R., and K. Hayakawa. 2015. Selection of natural autoreactive B cells. *Clin. Exp. Rheumatol.* 33(4, Suppl 92):S80–S86.

Hashimoto, S., A. Iwamatsu, M. Ishiai, K. Okawa, T. Yamadori, M. Matsushita, Y. Baba, T. Kishimoto, T. Kurosaki, and S. Tsukada. 1999. Identification of the SH2 domain binding protein of Bruton's tyrosine kinase as BLNK--functional significance of Btk-SH2 domain in B-cell antigen receptor-coupled calcium signaling. *Blood.* 94:2357–2364.

Havrylov, S., M.J. Redowicz, and V.L. Buchman. 2010. Emerging roles of Ruk/CIN85 in vesicle-mediated transport, adhesion, migration and malignancy. *Traffic.* 11:721–731. https://doi.org/10.1111/j.1600-0854.2010.01061.x

Hayashi, K., R. Nittono, N. Okamoto, S. Tsuji, Y. Hara, R. Goitsuka, and D. Kitamura. 2000. The B cell-restricted adaptor BASH is required for normal development and antigen receptor-mediated activation of B cells. *Proc. Natl. Acad. Sci. USA.* 97:2755–2760. https://doi.org/10.1073/pnas.040575697

Jumaa, H., B. Wollscheid, M. Mitterer, J. Wienands, M. Reth, and P.J. Nielsen. 1999. Abnormal development and function of B lymphocytes in mice deficient for the signaling adaptor protein SLP-65. *Immunity.* 11:547–554. https://doi.org/10.1016/S1074-7613(00)80130-2

Kometani, K., T. Yamada, Y. Sasaki, T. Yokosuka, T. Saito, K. Rajewsky, M. Ishiai, M. Hikida, and T. Kurosaki. 2011. CIN85 drives B cell responses by linking BCR signals to the canonical NF-kappaB pathway. *J. Exp. Med.* 208:1447–1457. https://doi.org/10.1084/jem.20102665

Kühn, J., L.E. Wong, S. Pirkuliyeva, K. Schulz, C. Schwiegk, K.G. Fünfgeld, S. Keppler, F.D. Batista, H. Urlaub, M. Habeck, et al. 2016. The adaptor protein CIN85 assembles intracellular signaling clusters for B cell activation. *Sci. Signal.* 9:ra66. https://doi.org/10.1126/scisignal.aad6275

Minegishi, Y., J. Rohrer, E. Coustan-Smith, H.M. Lederman, R. Pappu, D. Campana, A.C. Chan, and M.E. Conley. 1999. An essential role for BLNK in human B cell development. *Science.* 286:1954–1957. https://doi.org/10.1126/science.286.5446.1954

Navarro, M.N., G. Nusspaumer, P. Fuentes, S. González-García, J. Alcain, and M.L. Toribio. 2007. Identification of CMS as a cytosolic adaptor of the human pTα chain involved in pre-TCR function. *Blood.* 110:4331–4340. https://doi.org/10.1182/blood-2007-06-094938

Niiro, H., S. Jabbarzadeh-Tabrizi, Y. Kikushige, T. Shima, K. Noda, S. Ota, H. Tsuzuki, Y. Inoue, Y. Arinobu, H. Iwasaki, et al. 2012. CIN85 is required for Cbl-mediated regulation of antigen receptor signaling in human B cells. *Blood.* 119:2263–2273. https://doi.org/10.1182/blood-2011-04-351965

Oellerich, T., V. Bremes, K. Neumann, H. Bohnenberger, K. Dittmann, H.H. Hsiao, M. Engelke, T. Schnyder, F.D. Batista, H. Urlaub, and J. Wienands.

2011. The B-cell antigen receptor signals through a preformed transducer module of SLP65 and CIN85. *EMBO J.* 30:3620–3634. https://doi.org/10.1038/emboj.2011.251

Pappu, R., A.M. Cheng, B. Li, Q. Gong, C. Chiu, N. Griffin, M. White, B.P. Sleckman, and A.C. Chan. 1999. Requirement for B cell linker protein (BLNK) in B cell development. *Science.* 286:1949–1954. https://doi.org/10.1126/science.286.5446.1949

Rawlings, D.J., D.C. Saffran, S. Tsukada, D.A. Largaespada, J.C. Grimaldi, L. Cohen, R.N. Mohr, J.F. Bazan, M. Howard, N.G. Copeland, et al. 1993. Mutation of unique region of Bruton's tyrosine kinase in immunodeficient XID mice. *Science.* 261:358–361. https://doi.org/10.1126/science.8332901

Rothstein, T.L., and T.D. Quach. 2015. The human counterpart of mouse B-1 cells. *Ann. N. Y. Acad. Sci.* 1362:143–152. https://doi.org/10.1111/nyas.12790

Shimokawa, N., K. Haglund, S.M. Hölter, C. Grabbe, V. Kirkin, N. Koibuchi, C. Schultz, J. Rozman, D. Hoeller, C.H. Qiu, et al. 2010. CIN85 regulates dopamine receptor endocytosis and governs behaviour in mice. *EMBO J.* 29:2421–2432. https://doi.org/10.1038/emboj.2010.120

Stepensky, P., B. Keller, M. Buchta, A.K. Kienzler, O. Elpeleg, R. Somech, S. Cohen, I. Shachar, L.A. Miosge, M. Schlesier, et al. 2013. Deficiency of caspase recruitment domain family, member 11 (CARD11), causes profound combined immunodeficiency in human subjects. *J. Allergy Clin. Immunol.* 131:477–85.e1. https://doi.org/10.1016/j.jaci.2012.11.050

Su, Y.W., Y. Zhang, J. Schweikert, G.A. Koretzky, M. Reth, and J. Wienands. 1999. Interaction of SLP adaptors with the SH2 domain of Tec family kinases. *Eur. J. Immunol.* 29:3702–3711. https://doi.org/10.1002/(SICI)1521-4141(199911)29:11%3C3702::AID-IMMU3702%3E3.0.CO;2-R

Take, H., S. Watanabe, K. Takeda, Z.X. Yu, N. Iwata, and S. Kajigaya. 2000. Cloning and characterization of a novel adaptor protein, CIN85, that interacts with c-Cbl. *Biochem. Biophys. Res. Commun.* 268:321–328. https://doi.org/10.1006/bbrc.2000.2147

Xu, S., J.E. Tan, E.P. Wong, A. Manickam, S. Ponniah, and K.P. Lam. 2000. B cell development and activation defects resulting in xid-like immunodeficiency in BLNK/SLP-65-deficient mice. *Int. Immunol.* 12:397–404. https://doi.org/10.1093/intimm/12.3.397